Published in final edited form as:
Biochemistry. 2013 June 18; 52(24): 4138–4148. doi:10.1021/bi400118m.

DNA A-tracts Are Not Curved in Solutions Containing High Concentrations of Monovalent Cations†

Earle Stellwagen[‡], **Justin P. Peters**[§], **L. James Maher III**[*,§], and **Nancy C. Stellwagen**[*,‡]

[‡]Department of Biochemistry, University of Iowa, Iowa City, Iowa 52242 United States

[§]Department of Biochemistry and Molecular Biology, Mayo Clinic College of Medicine, Rochester, Minnesota 55905 United States

Abstract

The intrinsic curvature of seven 98-base pair DNA molecules containing up to four centrally located A_6-tracts has been measured by gel and capillary electrophoresis as a function of the number and arrangement of the A-tracts. At low cation concentrations, the electrophoretic mobility observed in polyacrylamide gels and in free solution decreases progressively with the increasing number of phased A-tracts, as expected for DNA molecules with increasingly curved backbone structures. Anomalously slow electrophoretic mobilities are also observed for DNA molecules containing two pairs of phased A-tracts that are out of phase with each other, suggesting that out-of-phase distortions of the helix backbone do not cancel each other out. The mobility decreases observed for the A-tract samples are due to curvature, not cation binding in the A-tract minor groove, because identical free solution mobilities are observed for a molecule with four out-of-phase A-tracts and one with no A-tracts. Surprisingly, the curvature of DNA A-tracts is gradually lost when the monovalent cation concentration is increased to ~200 mM, regardless of whether the cation is a hydrophilic ion like Na^+, NH_4^+ or $Tris^+$ or a hydrophobic ion like tetrabutylammonium (TBA^+). The decrease of A-tract curvature with increasing ionic strength, along with the known decrease of A-tract curvature with increasing temperature, suggests that DNA A-tracts are not significantly curved under physiological conditions.

Keywords

DNA A-tracts; curvature; monovalent cations; gel electrophoresis; capillary electrophoresis; free solution mobility

DNA molecules containing A-tracts, runs of four or more contiguous adenine residues, are known to be curved if the A-tracts are repeated in phase with the helix screw (reviews: Refs. 1–4). A-tract-induced curvature of DNA is easily measured by electrophoresis, because

†**Funding**
This work was supported in part by Grant CHE0748271 from the Analytical and Surface Chemistry Program of the National Science Foundation (to N.C.S.) and by the Mayo Graduate School, the Mayo Foundation, and National Institutes of Health Grant GM075965 (to L.J.M.)

[*]**Corresponding Authors**: N.C.S.: telephone, (319) 335-7896; fax, (319) 335-9570; nancy-stellwagen@uiowa.edu., L.J.M.: telephone, (507) 284-9041; fax: (507) 284-2053; maher@mayo.edu..

Notes
The authors declare no competing conflicts of interest.

ASSOCIATED CONTENT
Supporting Information
Table S1. Electrophoretic mobilities observed for the A-tract samples in polyacrylamide gels and in free solution. This information is available free of charge via the Internet at http://pubs.acs.org.

curved DNA molecules migrate more slowly than random-sequence DNAs containing the same number of base pairs, both in polyacrylamide gels[5–9] and in free solution.[10–12] Transient electric birefringence measurements have shown that DNAs containing phased A-tracts are stably curved, not anisotropically flexible, in low ionic strength solutions.[13–17]

Recent NMR experiments utilizing residual dipolar couplings have shown that isolated A-tracts embedded in small DNA oligomers are intrinsically curved.[18–21] The curvature is delocalized; some bending of the helix backbone occurs within the A-tract, while other bends occur at ApT and TpA base pair steps and/or at junctions between the A-tracts and their flanking sequences.[19–21] DNA A-tracts usually have narrow minor grooves, propeller-twisted A·T base pairs and bifurcated hydrogen bonds across the major groove[18, 22–27] (but see Ref. 28).

Many experimental methods have been used to determine the A-tract bend angle, including NMR,[18–21] ligase-catalyzed cyclization,[29, 30] transient electric birefringence[13, 16, 17] and dichroism, [14] atomic force microscopy,[31] superhelix unwinding,[32,33] fluorescence polarization anisotropy,[34] small molecule FRET,[35] and molecular dynamics.[36] The apparent bend angle ranges from 9° to 23°, depending on the length and sequence of the A-tract, the type of cation(s) in the solution and the method used to measure curvature. The average bend angle obtained by these methods is 15° ± 5° per A-tract.

The relative importance of monovalent cation binding to the curvature of DNA A-tracts curvature has not been resolved.[37–39] High resolution x-ray diffraction,[40–43] and NMR[21, 44–46] studies have shown that monovalent cations can be found in the A-tract minor groove, partially displacing some of the water molecules in the "spine of hydration"[47] in that groove. Monovalent cation occupancy of the A-tract minor groove ranges from 10% to 50% for Na^+, Rb^+, Cs^+, and Tl^+ ions, depending on the method of measurement and the identity of the cation. In addition, Tl^+ and Cs^+ ions have been found in the A-tract major groove.[43, 48, 49] Some investigators have suggested that excess monovalent cation binding in the A-tract minor groove *causes* DNA backbone curvature[3, 44, 50] because of asymmetric neutralization of the phosphate residues on opposite sides of the helix.[51, 52] Others have suggested that both electrostatic and nonelectrostatic forces contribute to the conformation and stability of DNA A-tracts.[37, 38, 53] In agreement with the latter hypothesis, a recent microsecond MD simulation of the Drew-Dickerson dodecamer[47] has shown that the narrow minor groove intrinsic to the AATT sequence is further narrowed when a long-lived Na^+ ion is localized in the groove.[27]

In this work, the effect of different monovalent cations on A-tract-induced DNA curvature has been studied using six 98 base pair (bp) DNA molecules containing up to four centrally located A_6-tracts as the model system. A 98-bp DNA molecule without A-tracts was used as the control. The sequences of the various DNAs, along with their acronyms and predicted structures,[54, 55] are given in Figure 1. Curvature was analyzed by complementary free solution capillary electrophoresis (CE) and polyacrylamide gel electrophoresis experiments. The running buffers, or background electrolytes (BGEs), contained various concentrations of Na^+, $Tris^+$, NH_4^+ or tetrabutylammonium (TBA^+) ions. The differences in mobility between the A-tract samples and the control were found to be very similar in free solution and in polyacrylamide gels, indicating that the two types of electrophoresis experiments are equally sensitive to A-tract curvature. Surprisingly, A-tract -induced DNA curvature is reduced or eliminated when the cation concentration is increased to ~200 mM, possibly because of the increased flexibility of the DNA helix at high ionic strengths.[56, 57] The biological consequences of the results are discussed.

MATERIALS AND METHODS

DNA samples

The 98-bp DNA constructs used in this work have roughly equal numbers of each nucleotide base and differ only with respect to the number and arrangement of the A-tracts in the center of each fragment, as shown in Figure 1. Samples 0, 1, 2i, 3i, and 4i contain the indicated number of in-phase A_6-tracts. Sample 4o contains four out-of-phase A_6-tracts. Sample 2i/o (2 in/out) contains two pairs of in-phase A_6-tracts. However, the two pairs of A-tracts are separated by 15 residues, making them out-of-phase with each other.

The DNA constructs were sub-cloned using the pGEM-T Easy Vector System (Promega). The oligonucleotide primers LJM-4449 (5'-AGCCTAGCCTATGACATGAC) and LJM-4450 (5'-GAGGTGAGGTTGCATTGCAT) (Integrated DNA Technologies) were used to amplify the 98-bp fragments by polymerase chain reaction (PCR). PCR reactions (100 μL) included 20 ng plasmid template, 0.4 μM forward and reverse primers, 100 μg/mL BSA, *Taq* DNA polymerase buffer (Invitrogen), 2 mM $MgCl_2$, 0.2 mM each dNTP, and 5 U *Taq* DNA polymerase (Invitrogen). Cycle conditions were 98°C (3 min), 30 cycles of [94°C (30 s), 55°C (30 s), and 72°C (45 s)], followed by 72°C (5 min). Following PCR, the various 98-bp samples were purified using QIAquick PCR Purification Kit (Qiagen).

Gel electrophoresis

Polyacrylamide gels containing 5% total acrylamide (5% T) were cast and run in various buffers at room temperature (~25°C). For all experiments reported here, 14.5 by 22.5 cm slab gels were used with 1.5-mm spacers. To a 40% acrylamide and bisacrylamide solution 19:1 (BioRad) diluted in running buffer, 0.1% (v/v) N,N,N',N'-tetramethylethylenediamine (TEMED, Sigma) and 0.1% (w/v) freshly dissolved ammonium persulfate (Sigma) were separately added, and the gel mixture was slowly poured between glass plates. Gelation occurred within 5–15 min, and the gels were pre-electrophoresed for 20 min before the samples and 100-bp ladder (Invitrogen) were loaded. Using an electric field strength of 8–12 V/cm, the gels were run until markers had migrated 50 to 90% of the length of the gel. Following electrophoresis, the gels were stained with 1X Sybr Green I (Invitrogen) in running buffer for 20 min. Images were then obtained using a Typhoon FLA 7000 (GE Healthcare), and migration distances (50 micron/pixel) were measured from the digital images.

A stock buffer of 25X TBE (2.5 M Tris base, 2.75 M boric acid, 0.05 M EDTA, pH 8.3) was prepared along with 50 and 200 mM TBA-cacodylate buffers (50 or 200 mM tetrabutylammonium hydroxide and 50 or 200 mM cacodylic acid, pH 6.6). Since Tris base is half ionized at its pKa of 8.07 (25°C), the concentration of $Tris^+$ ions in the TBE buffers, calculated from the Henderson-Hasselbalch equation, ranged from 30 to 700 mM. The TBA^+ concentrations in the 50 mM and 200 mM TBA-cacodylate buffers were calculated to be 35 and 145 mM, respectively, since cacodylic acid is half ionized at its pKa of 6.27 (25°C). To avoid confusion in the following text, the running buffers (or BGEs) are described by the cation concentration in each buffer, not the concentration of the buffer anion or the ionic strength of the solution.

Capillary electrophoresis

The free solution mobilities of the DNA samples were measured with a Beckman Coulter P/ACE MDQ Capillary Electrophoresis System (Fullerton, CA), using methods described previously.[11, 58, 59] All measurements were made in the reverse polarity mode (anode on the detector side) with UV detection at 254 nm. The capillaries were coated internally with linear polyacrylamide (Polymicro Technologies, Phoenix, AZ) to minimize the

electroosmotic flow (EOF) of the solvent. Previous studies have shown that this internal coating does not affect the observed mobilities.[60] The capillaries were 31.1 ± 0.2 cm in length (20.9 ± 0.1 cm to the detector) and 75 μm in internal diameter, and were mounted in a liquid-cooled cassette thermostated at 20°C. The electric fields applied to the capillary ranged from 30 to 330 V/cm, depending on the buffer concentration; the current was always 60 μA or less. Under such conditions the observed mobilities are independent of the applied electric field.[59, 60] The DNA samples were injected hydrodynamically at 0.5 psi (0.0035 MPa) for 3s; the sample plug occupied ~2.6% of the capillary length.

Most BGEs used for the CE experiments contained diethylmalonate (DM) as the buffering anion and Na^+, $Tris^+$, NH_4^+ or TBA^+ as the cation. Stock solutions containing 0.4 or 0.5 M diethylmalonic acid [$(CH_3CH_2)_2C(COOH)_2$, (Sigma-Aldrich, St. Louis, MO)] were titrated to pH 7.3, the pKa of the second carboxyl group of diethylmalonic acid (25°), with a concentrated solution of the hydroxide of the cation of choice. The cation concentrations in the stock solutions were 0.6 or 0.75 M, because the second carboxyl group of diethylmalonic acid is half-ionized at pH 7.3. Tris-acetate buffer, pH 8.0, was prepared as described previously.[58] All BGEs are identified in the following text by the type of cation in the buffer and the cation concentration.

Calculation of mobility

The observed mobilities, μ_{obs}, of the DNA samples were calculated from eq 1:

$$\mu_{obs}=L_d/E_t \quad (1)$$

where L_d is the distance migrated in the gel or the distance from the inlet of the capillary to the detector in cm, t is the migration time in seconds, and E is the applied electric field in V/cm.

In capillary electrophoresis, the observed mobilities correspond to the algebraic sum of the actual mobility of the DNA, μ and the mobility caused by the electroosmotic flow (EOF) of the solvent, μ_{EOF}. Although the internally coated capillaries used in the present experiments have very low EOF, the observed mobility can and does vary slightly from one run to another because of transient changes in the capillary coating. Changes in μ_{EOF} were monitored by including a small single-stranded DNA oligomer in each solution as a marker, calculating the average mobility of the marker in a given series of experiments and normalizing the observed mobilities to the average mobility of the marker.[59–62] These EOF-corrected mobilities are called normalized mobilities in the following text. Two different oligomers, with the sequences ACCTG and ACCTGAT, were used as markers. Since the normalized mobilities of the A-tract samples were independent of which marker was used, the markers are not specifically identified in the following text.

The mobilities of the various A-tract samples are reported as the difference in mobility ($\Delta\mu$) between an A-tract sample and a control, usually sample 0. Using sample 4i as an example, $\Delta\mu = \mu(4i) - \mu(0)$. The mobility differences are negative in sign because the mobilities observed for the A-tract samples are smaller than the mobility of the control. For convenience, all mobilities and mobility differences are reported in mobility units, m.u. (1 m.u. = 1×10^{-4} cm^2/Vs).

The anomalously slow electrophoretic mobilities of A-tract DNAs have often been characterized by the ratio of the apparent length of the curved DNA (determined by comparison with DNA markers) to its sequence length.[6, 7, 9, 51, 63] In the present case, an

equivalent way of presenting the data would be to calculate the ratio of the mobility of an A-tract DNA to the mobility of a control. The mobility ratios (not shown) have been calculated for all experiments described here and exhibit the same trends as the mobility differences illustrated below in Figures 3 to 6. However, the mobility ratios obtained in polyacrylamide gels and in free solution differ somewhat in magnitude, due in part to the different anions used in the BGEs[108, 109] and in part to interactions between curved DNAs and the polyacrylamide gel matrix.[110–112] The mobility ratios obtained in polyacrylamide gels and in free solution can be made to coincide by multiplying one of the data sets by a small constant factor. However, this procedure is arbitrary and obscures the similarity of the mobility differences observed in gels and in free solution. Therefore, we have presented our results in terms of the mobility differences. For the interested reader, the actual mobilities observed in polyacrylamide gels and the normalized mobilities observed in free solution are given in Table S1 in the Supplementary Information.

RESULTS

Electropherograms

A typical CE electropherogram observed for sample 4i in a solution containing 100 mM NH_4^+ ions is illustrated in Figure 2A. The peak on the left corresponds to sample 4i, while the peak on the right corresponds to the marker ACCTGAT. Both peaks are monodisperse and approximately Gaussian in shape. Similar CE electropherograms were observed for the other A-tract samples studied here.

Typical electropherograms observed for the A-tract samples in polyacrylamide gels cast and run in different buffers are illustrated in Figure 2B. The buffers contained 30 mM $Tris^+$ (left), 110 mM $Tris^+$(center), or 145 mM TBA^+ (right). The mobilities observed for samples 1, 2i, 3i, and 4i in 30 mM $Tris^+$ buffer (left electropherogram) decreased progressively with the increasing number of in-phase A-tracts, as expected from previous studies.[1, 2, 6, 9, 63] However, the mobility differences between samples were markedly reduced in BGEs containing 110 mM $Tris^+$ or 145 mM TBA^+, as shown in the center and right electropherograms.

Hydrophilic cations

The mobilities observed for the various A-tract samples in polyacrylamide gels and in free solution are most easily compared by calculating the difference in mobility between the A-tract samples and sample 0, with no A-tracts. The mobility differences observed in polyacrylamide gels and in free solution using BGEs containing 30 or 20 mM $Tris^+$, respectively, are compared in Figure 3. Somewhat surprisingly, the mobility differences observed in gels and in free solution are comparable in magnitude. The increase in the absolute magnitude of the mobility differences with the increasing number of in-phase A-tracts could be due to differences in effective charge and/or differences in shape. Differences in effective charge would occur if the A-tracts were to bind excess monovalent cations in the minor groove, decreasing the effective net charge and thereby decreasing the mobility.[11, 12] If the mobilities of the A-tract samples were determined primarily by differences in effective charge, the mobility differences observed for samples 4i, 2i/o and 4o should have been equal since each contains four A-tracts. The significant mobility differences observed for these three samples indicate that the mobilities are determined primarily by differences in shape.

The gradual increase in the absolute value of the mobility differences observed for samples 1, 2i, 3i and 4i is consistent with a progressive increase in backbone curvature with the number of phased A-tracts, as depicted graphically in Figure 1B and as expected from previous studies in the literature.[1–12] The mobility difference observed for sample 2i/o,

which contains two pairs of in-phase A-tracts that are out-of-phase with each other, lies between the mobility differences observed for samples 2i and 3i. Hence, as also shown in Figure 1B, A-tract-induced backbone curvature cannot be eliminated by placing curved sequence elements on opposite sides of the DNA helix.

The variation of the mobility differences observed for the A-tract samples with cation concentration is illustrated in Figure 4. The mobility differences decreased in absolute magnitude with increasing [NH_4^+] in free solution (Figure 4A) and with increasing [$Tris^+$] in polyacrylamide gels (Figure 4B). The results are consistent with a previous study in polyacrylamide gels, which showed that the anomalously slow mobilities of A-tract DNAs decreased when NaCl was added to TBE buffer.[8, 9] Importantly, Figure 4 also shows that the mobility differences observed for sample 4o, with four out-of-phase A-tracts and sample 0, with no A-tracts, are equal within experimental error. Therefore, the slower mobilities observed for the A-tract samples in free solution and in polyacrylamide gels must be attributed primarily to hydrodynamic effects that are caused by differences in shape.

The dependence of the mobility differences on cation concentration is illustrated in more detail in Figure 5A, where the mobility differences observed between samples 4i and 4o are plotted as a function of cation concentration. Sample 4o was chosen as the control for this comparison, rather than sample 0, because samples 4i and 4o each contain four A-tracts. Hence, any preferential cation binding in the A-tract minor groove would be the same for both DNAs. The mobility differences observed in free solution, using either NH_4^+ or Na^+ as the cation, and in polyacrylamide gels, using $Tris^+$ as the cation, decrease in absolute magnitude with increasing cation concentration until leveling off and becoming constant at a cation concentration of ~200 mM. The plateau value of the mobility difference is −0.110 m.u.; the midpoint of the transition occurs at 107 ± 7 mM. At the physiological monovalent cation concentration of ~140 mM, the mobility difference between samples 4i and 4o decreased to ~15% of the value observed at cation concentrations lower than ~50 mM.

Hydrophobic cations

The mobility differences observed for the various A-tract samples in BGEs containing the bulky tetrabutylammonium ion (TBA^+) as the only cation in the solution are illustrated in Figure 6. In both polyacrylamide gels and in free solution, the mobility differences are independent of the number and arrangement of the A-tracts when the TBA^+ concentration is 100 mM or greater. The mobility differences observed between samples 4i and 4o are plotted as a function of TBA^+ concentration in Figure 5B. As observed with the hydrophilic cations in Figure 5A, the mobility differences decreased in absolute magnitude with increasing TBA^+ concentration until becoming equal to zero at a TBA^+ concentration of ~200 mM. The midpoint of the transition occurs at 73 ± 12 mM TBA^+.

The similarity of the results obtained in solutions containing both hydrophilic and hydrophobic cations suggests that DNA A-tracts become less curved with increasing ionic strength. Surprisingly, however, the plateau mobility differences depend on whether the cation is hydrophilic or hydrophobic, as shown by comparing Figures 5A and 5B. The small but finite mobility difference observed for sample 4i in solutions containing high concentrations of Na^+, NH_4^+, or $Tris^+$ ions suggests that DNA A-tracts retain a small amount of residual curvature in such solutions, whereas in TBA^+ the residual curvature is lost.

DISCUSSION

Effective charge of A-tract DNAs

The work described here has shown that DNA molecules containing phased A-tracts migrate anomalously slowly in free solution as well as in polyacrylamide gels. Because the free solution mobilities are identical for sample 0, with no A-tracts, and sample 4o, with four out-of-phase A-tracts, the mobility differences are not due to differences in effective charge caused by preferential cation binding in the A-tract minor groove . Even if some preferential counterion binding were to occur, the change in the net charge of the DNA would be virtually undetectable, since the DNA samples contain 98 base pairs and one to four A-tracts, each of which would be only partially occupied by a monovalent cation. [12, 37, 40–43, 64, 65] Therefore, the mobility differences observed for the various A-tract samples must be due primarily to differences in shape.

A-tract-induced curvature of the DNA helix axis

An important question to be answered is whether the free solution mobility differences observed for the different A-tract samples can be explained by hydrodynamic effects due to differences in shape. Since rotational diffusion is much faster than translational diffusion, the migrating DNA molecules will sample all possible orientations during free solution electrophoresis. [66, 67] Therefore, the free solution mobility, μ, will be determined by the effective charge of the DNA, Q, which interacts with the electric field to provide the driving force for electrophoresis, and the translational diffusion coefficient, D_t, which characterizes the friction between the migrating DNA molecules and the solvent.[68] The relationship between these two variables is shown in eq 2:

$$\mu = Q D_t N^{-0.67} / k_B T \quad (2)$$

where N is the number of base pairs in the DNA, k_B is Boltzmann's constant and T is the absolute temperature. The factor $N^{-0.67}$ compensates for the fact that the mobilities of large DNA molecules are independent of molecular weight while the diffusion coefficients decrease as the 0.67 power of molecular weight.[69] In relatively low electric fields, such as those used in the present study, cations in the condensed ion layer migrate with the DNA,[68, 70–76] making Q equal to the effective charge of the phosphate residues after counterion condensation, [77, 78] not the total number of charged phosphate residues. Hence, the effective charge of the various DNA samples is 0.24 times the number of bases.[77] As discussed above, Q is essentially independent of the presence or absence of A-tracts in the samples studied here.

Garcia de la Torre and coworkers[79] have derived an expression for the translational diffusion coefficients of linear DNA molecules, as shown in eq 3:

$$D_t = \frac{k_B T}{3\pi\eta_o L}[\ln p + 0.312 + 0.565/p] \quad 3$$

Here, η_o is the viscosity of the solvent, L is the end-to-end length of the DNA and p is the axial ratio (length/diameter). Previous studies have shown that the diffusion coefficients calculated for linear DNAs from eq 3 are very close to the experimentally measured values.[69] For a DNA molecule without A-tracts, like sample 0, or with out-of-phase A-tracts like sample 4o, L can be approximated as 3.4 Å/ bp × 98 bp or 333 Å. If the diameter of the DNA is taken to be 25, Å, [79, 80] p = 13.3 and D_t is calculated to be 3.79 ×10^{-7} cm^2/s at 20°C from eq 3.

In order to estimate the diffusion constant of sample 4i, for comparison with that of the controls, it is necessary to estimate the length and axial ratio of this DNA. If the dimensions of sample 4i are approximated from the structure illustrated in Figure 1B, the approximate end-to-end length is 283 Å. An important question is how to estimate the diameter of sample 4i. Most investigators who have studied the translational diffusion coefficients of bent rods have tacitly assumed that the diameters of bent and straight rods are equal.[81–84] If we assume that the diameter of sample 4i is equal to 25 Å and take the length to be 283 Å, as suggested by Figure 1B, the axial ratio is calculated to be 11.3, and D_t is calculated to be 4.22×10^{-7} cm^2/s, larger than the diffusion coefficient calculated for the control. From eq 2, an increase in the translational diffusion constant of sample 4i would lead to an *increase* in the observed mobility, just the *opposite* of the observed results. Similar results are obtained if the mobilities are calculated from radii of gyration of the curved and straight DNAs.

Therefore, in order to explain the experimental results, it must be assumed that curved DNAs migrate through the solution essentially as ellipsoids of revolution, with maximum dimensions approximately equal to the length and effective diameter of the curved molecule.[113] The effective diameter of sample 4i would then correspond to the arc subtended by the ends of the curved rod in Figure 1B. With this diameter, and assuming the effective length to be 283 Å, the axial ratio is calculated to be 3.5 and the diffusion coefficient estimated from eq 3 is 2.73×10^{-7} cm^2/s at 20°C.

Alternatively, sample 4i could be approximated as a once-broken rod with a central bend corresponding to the cumulative bend induced by four in-phase A-tracts. Taking the average A-tract bend angle to be 15°, the average of the experimentally determined values (see above), a once-broken rod with a central bend of 60° (4 × 15°) is estimated to have an end-to-end length of ~270 Å and an axial ratio of ~3.2. The translational diffusion coefficient calculated for such a structure from eq 3 is 2.08×10^{-7} cm^2/s at 20°C. A similar translational diffusion coefficient is calculated for a twice-broken rod with a virtual bend of 60° between the two legs. Hence, it seems reasonable to approximate the diffusion constant of sample 4i as $(2.4 \pm 0.3) \times 10^{-7}$ cm /s. The difference in the diffusion constants, ΔD_t, between samples 4i and 4o (or between samples 4i and 0) is then calculated to be $\sim 1.4 \times 10^{-7}$ cm^2 /s.

If the effective charge per base is 0.24 after counterion condensation[77], $Q = 0.24 \times N_o \times e_o$, where N_o is the number of phosphate residues and e_o is the electronic charge of the proton. Substituting these values into eq 2,the difference in mobility between samples 4i and 4o (or between samples 4i and 0) is calculated to be:

$$\Delta\mu = \frac{0.24 e_o N_o \Delta D_t N^{-0.67}}{k_B T} \quad 4$$

Evaluating the factor e_0/k_BT as 39.6 V^{-1} at 20°C, remembering that N_o (the number of phosphate residues) is 196 and N (the number of base pairs) is 98, and using the ΔD_t value calculated above (1.4×10^{-7} cm^2/s), the mobility difference between samples 4i and 4o (or between samples 4i and 0) is calculated to be 0.12 m.u. The observed mobility difference between samples 4i and 4o was found to be 0.046 m.u. in a BGE containing 10 mM $NH4^+$ (Figure 4A). The calculated and observed mobility differences agree within a factor of three, which is satisfactory given the approximate nature of the calculation. Hence, the mobility differences observed in free solution can be explained by differences in shape between the curved and straight DNAs. In future work, we plan to compare more precise calculations of the translational diffusion coefficients of the A-tract DNAs with their free solution mobilities to determine whether curved DNA molecules effectively migrate through the solution as ellipsoids of revolution.

Decrease of A-tract curvature with increasing cation concentration

The most surprising result obtained in the present studies is the gradual loss of A-tract curvature with increasing monovalent cation concentration (Figures 5A and 5B). Because similar results were observed in BGEs containing Na^+, NH_4^+, $Tris^+$ or TBA^+ ions, the decrease of A-tract-induced curvature of the helix backbone appears to be an ionic strength effect that is relatively independent of cation identity. The small difference in the midpoints of the conformational transitions observed with the hydrophilic cations and with TBA^+ may be due to electrostatic effects that vary with cation size.[85] Similar electrostatic effects may contribute to the small plateau mobility differences observed in BGEs containing hydrophilic cations and TBA^+. Further studies are underway to investigate these questions.

The decrease in curvature observed at high cation concentrations implies that DNA A-tracts are conformationally flexible. At low cation concentrations, the A-tracts appear to be *inherently curved*, in agreement with recent high resolution NMR experiments[18–21] and MD simulations.[36] The intrinsic curvature is not caused by monovalent cation binding in the A-tract minor groove, because the curvature should then be increased at high cation concentrations, not reduced. The decrease in A-tract curvature with increasing monovalent cation concentration could be due to a variety of causes, none of them mutually exclusive:

1) Conformational differences at different cation concentrations—Imino proton magnetic resonance experiments by Leroy and coworkers[86, 87] have shown that the lifetimes of the A·T base pairs in DNA A-tracts are much longer than those observed for isolated A·T base pairs or for G·C base pairs. The anomalously long base pair lifetimes observed for the A·T base pairs in DNA A-tracts become shorter at high NH_4^+ ion concentrations, suggesting that the A-tracts have somewhat different structures and/or flexibilities at high and low ionic strengths. Similar variations in DNA conformation with increasing NH_4^+ concentration have been observed by others.[88]

2) Changes in the counterion cloud with increasing cation concentration—Since DNA is a highly charged polyelectrolyte, it is surrounded by a dense cloud of condensed counterions.[77, 78, 89, 90] Outside the counterion cloud is a layer of solvent enriched in coions, which in turn is surrounded by the ions in the Debye layer.[91, 92] MD studies,[93] all-atom energy simulations,[94] and model-based calculations[95–97] have shown that cations are concentrated on the concave side of the DNA helix when the bend angle is large, screening the repulsion of the phosphate residues. As the ionic strength of the solution is increased, the thickness of the Debye layer approaches the thickness of the condensed counterion layer, leading to a modest increase in the local density of condensed counterions on all sides of the helix.[73, 91] Under such conditions, A-tract and non-A-tract phosphate residues might experience the same electrostatic environment, leading to equalization of charge repulsion and straightening of the helix backbone.

3) An increase in the flexibility of DNA at high salt concentrations—It has been known for many years that the flexibility of DNA increases with increasing ionic strength.[56, 57, 98, 99] Increased flexibility would be expected to be observed for both A-tract and non-A-tract base pairs. If the flexibility of all base pairs was similar at high salt concentrations, as suggested by the normalization of the base-pair lifetimes in DNA A-tracts,[86, 87] the conformations of DNAs with and without A-tracts would be expected to become essentially equal at high cation concentrations, straightening the helix backbone. Further studies will be needed to differentiate among these possibilities.

Biological implications

The overabundance of A-tracts in the eukaryotic genome,[100] the frequent occurrence of A-tracts near transcription start sites and origins of replication,[4] and the periodic pattern of AAA and AAT trinucleotides in nucleosomal DNA[101, 102] all suggest that DNA A-tracts have important biological functions in the cell. However, A-tract curvature is reduced by ~85% when the monovalent cation concentration is increased to approximately physiological levels at 20°C (this work), and by increasing the temperature to the physiologically relevant temperature of 37°C.[102–107] Therefore, it seems unlikely that DNA A-tracts are significantly curved in the cell. Other properties of DNA A-tracts, such as the increased stiffness[4, 24, 36] and/or the enhanced electronegativity of the minor groove.[114] might contribute to the biological function of DNA A-tracts. Alternatively, A-tract-induced curvature of the helix backbone could be relevant if the A-tracts exist in a variety of conformations and the fractional population of curved structures is enhanced by coupled equilibria with other components in the cell.

Supplementary Material

Refer to Web version on PubMed Central for supplementary material.

Acknowledgments

The authors thank Nicole Becker for advice and discussions.

Abbreviations

BGE	background electrolyte
CE	capillary electrophoresis
EOF	electroosmotic flow
MD	molecular dynamics
m.u.	mobility unit (1 m.u. = 1×10^{-4} cm^2/Vs
TBA	tetrabutylammonium
TBE	Tris-borate-EDTA
μ	mobility

REFERENCES

1. Hagerman PJ. Sequence-directed curvature of DNA. Annu. Rev. Biochem. 1990; 59:755–781. [PubMed: 2197990]
2. Olson, WK.; Zhurkin, VB. Twenty years of DNA bending. In: Sarma, RH.; Sarma, MH., editors. In Biological Structure and Dynamics. NY: Adenine Press,Schenectady; 1996. p. 341-370.
3. Hud NV, Plavec J. A unified model for the origin of DNA sequence-directed curvature. Biopolymers. 2003; 69:144–159. [PubMed: 12717729]
4. Haran TE, Mohanty U. The unique structure of A-tracts and intrinsic DNA bending. Quar. Rev. Biophys. 2009; 42:41–81.
5. Wu M-M, Crothers DM. The locus of sequence-directed and protein-induced DNA bending. Nature. 1984; 308:509–513. [PubMed: 6323997]
6. Koo H-S, Wu H-M, Crothers DM. DNA bending at adenine·thymine tracts. Nature. 1986; 320:501–506. [PubMed: 3960133]
7. Hagerman PJ. Sequence-directed curvature of DNA. Nature. 1986; 321:449–450. [PubMed: 3713816]

8. Diekmann S, Wang JC. On the sequence determinants and flexibility of the kinetoplast DNA fragment with abnormal gel electrophoretic mobilities. J. Mol. Biol. 1985; 186:1–11. [PubMed: 3001314]
9. Diekmann S. Temperature and salt dependence of the gel migration anomaly of curved DNA fragments. Nucleic Acids Res. 1987; 15:247–265. [PubMed: 3029673]
10. Stellwagen E, Lu YJ, Stellwagen NC. Curved DNA molecules migrate anomalously slowly in free solution. Nucleic Acids. Res. 2005; 33:4425–4432. [PubMed: 16085753]
11. Dong Q, Stellwagen E, Stellwagen NC. Monovalent cation binding in the minor groove of DNA A-tracts. Biochemistry. 2009; 48:1047–1055. [PubMed: 19154116]
12. Lu YJ, Stellwagen NC. Monovalent cation binding by curved DNA molecules containing variable numbers of A-tracts. Biophys J. 2008; 94:1719–1725. [PubMed: 17993492]
13. Hagerman PJ. Evidence for the existence of stable curvature of DNA in solution. Proc. Natl. Acad. Sci. USA. 1984; 81:4632–4636. [PubMed: 6087336]
14. Levene SD, Wu H-M, Crothers DM. Bending and flexibility of kinetoplast DNA. Biochemistry. 1986; 25:3988–3995. [PubMed: 3017412]
15. Stellwagen NC. Transient electric birefringence of two small DNA restriction fragments of the same molecular weight. Biopolymers. 1991; 31:1651–1667. [PubMed: 1814510]
16. Lu YJ, Weers BD, Stellwagen NC. Analysis of DNA bending by transient electric birefringence. Biopolymers. 2003; 70:270–288. [PubMed: 14517915]
17. Lu YJ, Weers BD, Stellwagen NC. Intrinsic curvature in the VP1 gene of SV40: comparison of solution and gel results. Biophys J. 2005; 88:1191–1206. [PubMed: 15556988]
18. Macdonald D, Herbert K, Zhang X, Polgruto T, Lu P. Solution structure of an A-tract DNA bend. J. Mol. Biol. 2001; 306:1081–1098. [PubMed: 11237619]
19. Wu Z, Delaglio F, Tjandra N, Zhurkin VB, Bax A. Overall structure and sugar dynamics of a DNA dodecamer from homo- and heteronuclear dipolar couplings and ^{31}P chemical shift anisotropy. J. Biomol. NMR. 2003; 26:297–315. [PubMed: 12815257]
20. Barbič A, Zimmer DP, Crothers DM. Structural origins of adenine-tract bending. Proc. Natl. Acad. Sci. USA. 2003; 100:2369–2373. [PubMed: 12586860]
21. Stefl R, Wu H, Ravindranathan S, Sklenář, Feigon J. DNA A-tract bending in three dimensions: solving the dA_4T_4 vs. dT_4A_4 conundrum. Proc. Natl. Acad. Sci. USA. 2004; 101:1177–1182. [PubMed: 14739342]
22. Nelson HCM, Finch JT, Luisi BF, Klug A. The structure of an oligo(dA)·oligo(dT) tract and its biological implications. Nature. 1987; 330:221–226. [PubMed: 3670410]
23. Coll M, Frederick CA, Wang AH-J, Rich A. A bifurcated hydrogenbonded conformation in the d(A·T) base pairs of the DNA dodecamer d(CGCAAATTTGCG) and its complex with distamycin. Proc. Natl. Acad. Sci. USA. 1987; 84:8385–8389. [PubMed: 3479798]
24. Yoon C, Privé GG, Goodsell DS, Dickerson RE. Structure of an alternating-B DNA helix and its relationship to A-tract DNA. Proc. Natl. Acad. Sci. USA. 1988; 85:6332–6226. [PubMed: 3413099]
25. Hizver J, Rozenberg H, Frolow F, Rabinovich D, Shakked Z. DNA bending by an adenine-thymine tract and its role in gene regulation. Proc. Natl. Acad. Sci. USA. 2001; 98:8490–8495. [PubMed: 11438706]
26. DiGabriele AD, Steitz TA. A DNA dodecamer containing an adenine tract crystallizes in a unique lattice and exhibits a new bend. J. Mol. Biol. 1993; 231:1024–1039. [PubMed: 8515463]
27. Pérez A, Luque FJ, Orozco M. Dynamics of B-DNA on the microsecond time scale. J. Am. Chem. Soc. 2007; 129:14729–14745.
28. Maehigashi T, Hsiao C, Woods KK, Moulaei T, Hud NV, Williams LD. B-DNA structure is intrinsically polymorphic: even at the level of base pair positions. Nucleic Acids Res. 2012; 40:3714–3722. [PubMed: 22180536]
29. Koo H-S, Drak J, Rice JA, Crothers DM. Determination of the extent of DNA bending by an adenine-thymine tract. Biochemistry. 1990; 29:4227–4234. [PubMed: 2361140]
30. Du Q, Vologodskaia M, Kuhn H, Frank-Kamenetskii F, Vologodskii A. Gapped DNA and cyclization of short DNA fragments. Biophys. J. 2005; 88:4137–4145. [PubMed: 15778443]

31. Rivetti C, Walker C, Bustamante C. Polymer chain statistics and conformational analysis of DNA molecules with bends or sections of different flexibility. Proc. Natl. Acad. Sci. USA. 1998; 280:41–59.
32. Tchernaenko V, Halvorson HR, Lutter LC. Topological measurement of an A-tract bend angle: variation of duplex winding. J. Mol. Biol. 2003; 326:751–760. [PubMed: 12581637]
33. Tchernaenko V, Radlinska M, Drabik C, Bujnicki J, Halvoraon HR, Lutter LC. Topological measurement of an A-tract bend angle: comparison of the bent and straightened states. J. Mol. Biol. 2003; 326:737–749. [PubMed: 12581636]
34. Chirico G, Collini M, Tóth K, Brun N, Langowski J. Rotational dynamics ofcurved DNA fragments studied by fluorescence polarization anisotropy. Eur. Biophys. J. 2001; 29:597–606. [PubMed: 11288835]
35. Wozniak AK, Schröder GF, Grubmüller H, Seidel CAM, Oesterhelt F. Single-molecule FRET measures bends and kinks in DNA. Proc. Natl. Acad. Sci. USA. 2008; 105:18337–18342. [PubMed: 19020079]
36. Lankaš F, Špačková N, Moakher M, Enkhbayar P, Šponer J. A measure of bending in nucleic acids structures applied to A-tract DNA. Nucleic Acids Res. 2010; 38:3414–3422. [PubMed: 20123729]
37. Egli M. DNA-cation interactions: quo vadis? Chem. Biol. 2002; 9:277–288. [PubMed: 11927253]
38. Subirana JA, Soler-López M. Cations as hydrogen bond donors: a view of electrostatic interactions in DNA. Annu. Rev. Biophys. Biomol. Struct. 2003; 32:27–45. [PubMed: 12598364]
39. Egli M. Nucleic acid crystallography: current progress. Curr. Opin. Chem. Biol. 2004; 8:580–591. [PubMed: 15556400]
40. Sines CC, McFail-Isom L, Howerton SB, VanDerveer D, Williams LD. Cations mediate B-DNA conformational heterogeneity. J. Am. Chem. Soc. 2000; 122:11048–11056.
41. Tereshko V, Minasoc G, Egli M. A “hydrat-ion” spine in a B-DNA minor groove. J. Am Chem. Soc. 1999; 121:3590–3595.
42. Woods KK, McFail-Isom L, Sines CC, Howerton SB, Stephens RK, Williams LD. Monovalent cations sequester within the A-tract minor groove of $[d(CGCGAATTCGCG)]_2$. J. Am. Chem. Soc. 122:1546–1547.
43. Howerton SB, Sines CC, VanDerveer D, Williams LD. Locating monovalent cations in the grooves of B-DNA. Biochemistry. 2001; 40:10012–10031.
44. Hud NV, Sklenář V, Feigon J. Localization of ammonium ions in the minor groove of DNA duplexes in solution and the origin of A-tract bending. J. Mol. Biol. 1999; 286:651–660. [PubMed: 10024440]
45. Marincola FC, Denisov VP, Halle B. Competitive Na^+ and Rb^+ binding in the minor groove of DNA. J. Am. Chem. Soc. 2004; 126:6739–6750. [PubMed: 15161302]
46. Denisov VP, Halle B. Sequence-specific binding of counterions to*B*-DNA. Proc. Natl. Acad. Sci. USA. 2000; 97:629–633. [PubMed: 10639130]
47. Drew HR, Dickerson RE. Structure of a B-DNA dodecamer. III. Geometry of hydration. J. Mol. Biol. 1981; 151:535–556. [PubMed: 7338904]
48. Watkins D, Mohan S, Koudelka GB, Williams LD. Sequence recognition of DNA by protein-induced conformational transitions. J. Mol. Biol. 2009; 396:1145–1164. [PubMed: 20053356]
49. Bartenev VM, Golovamov EuI, Kapitonova KA, Mokulskii MA, Volkova LI, Skuratovskii IYa. Structure of the *B* DNA cationic shell as revealed by an x-ray diffraction study of CsDNA. J. Mol. Biol. 1983; 169:217–234. [PubMed: 6620381]
50. Hamelberg D, McFail-Isom L, Williams LD, Wilson WD. Flexible structure of DNA: ion dependence of minor-groove structure and dynamics. J. Am. Chem. Soc. 2000; 122:10513–10520.
51. Strauss JK, Maher LJ III. DNA bending by asymmetric phosphate neutralization. Science. 1994; 266:1829–1834. [PubMed: 7997878]
52. Williams LD, Maher LJ III. Electrostatic mechanisms of DNA deformation. Annu. Rev. Biophys. Biomol. Struct. 2000; 29:497–521. [PubMed: 10940257]
53. Beveridge DL, Dixit SB, Barreiro G, Thayer KM. Molecular dynamics simulations of DNA curvature and flexibility: helix phasing and premelting. Biopolymers. 2004; 73:380–403. [PubMed: 14755574]

54. Vlahoviček K, Kaján L, Pongor S. DNA analysis servers: plot.it, bend.it, model.it and IS. Nucleic Acids Res. 2003; 31:3686–3687. http://hydra.icgeb.trieste.it/dna/index.php. [PubMed: 12824394]
55. Gabrielian A, Pongor S. Correlation of intrinsic DNA curvature with DNA property periodicity. FEBS Lett. 1996; 393:65–68. [PubMed: 8804425]
56. Odijk T, Houwaart AC. On the theory of the excluded-volume effect of apolyelectrolyte in a 1-1 electrolyte solution. J. Polym Sci: Polym. Phys. Ed. 1978; 16:627–639.
57. Baumann CG, Smith SB, Bloomfield VA, Bustamanti C. Ionic effects on the elasticity of single DNA molecules. Proc. Natl Acad. Sci. USA. 1997; 94:6185–6190. [PubMed: 9177192]
58. Dong Q, Stellwagen E, Dagle JM, Stellwagen NC. Free solution mobility of small single-stranded oligonucleotides with variable charge densities. Electrophoresis. 2003; 24:3323–3329. [PubMed: 14595678]
59. Stellwagen E, Dong Q, Stellwagen NC. Quantitative analysis of monovalent counterion binding to random-sequence, double-stranded DNA using the replacement ion method. Biochemistry. 2007; 46:2050–2058. [PubMed: 17253778]
60. Stellwagen NC, Gelfi C, Righetti PG. The free solution mobility of DNA. Biopolymers. 1997; 42:687–703. [PubMed: 9358733]
61. Stellwagen E, Abdulla A, Dong Q, Stellwagen NC. Electrophoretic mobility is a reporter of hairpin structure in single-stranded DNA oligomers. Biochemistry. 2007; 46:10931–10941. [PubMed: 17764160]
62. Chang CY, Stellwagen NC. Tandem GA residues on opposite sides of the loop in molecular beacon-like DNA hairpins compact the loop and increase hairpin stability. Biochemistry. 2011; 50:9148–9157. [PubMed: 21942650]
63. Hagerman PJ. Sequence dependence of the curvature of DNA: a test of the phasing hypothesis. Biochemistry. 1985; 24:7033–7037. [PubMed: 4084556]
64. Young MA, Jayaram B, Beveridge DL. Intrusion of counterions into the spine of hydration in the minor groove of B-DNA: fractional occupancy of electronegative pockets. J. Am. Chem. Soc. 1997; 119:59–69.
65. Várnal P, Zakrzewska K. DNA and its counterions: a molecular dynamics study. Nucleic Acids Res. 2004; 32:4269–4280. [PubMed: 15304564]
66. Stellwagen NC, Bossi A, Gelfi C, Righetti PG. Do orientation effects contribute to the molecular weight dependence of the free solution mobility of DNA? Electrophoresis. 2001; 22:4311–4315. [PubMed: 11824595]
67. Li ZR, Liu GR, Chen YZ, Wang J-S, Bow H, Cheng Y, Han J. Continuum transport model of Ogston sieving in patterned nanofilter arrays for separation of rod-like biomolecules. Electrophoresis. 2008; 29:329–339. [PubMed: 18203240]
68. Viovy J-L. Electrophoresis of DNA and other polyelectrolytes: physical mechanisms. Rev. Mod. Phys. 2000; 72:813–872.
69. Stellwagen E, Lu YJ, Stellwagen NC. Unified description of electrophoresis and diffusion for DNA and other polyions. Biochemistry. 2003; 42:11745–11750. [PubMed: 14529285]
70. Ma C, Bloomfield VA. Gel electrophoresis measurement of counterion condensation on DNA. Biopolymers. 1994; 35:211–216. [PubMed: 7696566]
71. Li AZ, Qi LJ, Shih HH, Marx KA. Trivalent counterion condensation of DNA measured by pulse gel electrophoresis. Biopolymers. 1995; 38:367–376. [PubMed: 8906972]
72. Li A, Huang H, Re X, Qi LJ, Marx KA. A gel electrophoresis study of the competitive effects of monovalent counterion on the extent of divalent counterions binding to DNA. Biophys. J. 1998; 74:964–973. [PubMed: 9533707]
73. Grass K, Holm C. Mesoscale modeling pf polyelectrolyte electrophoresis. Faraday Discuss. 2010; 144:57–70. [PubMed: 20158023]
74. Frank S, Winkler RG. Mesoscale hydrodynamic simulation of short polyelectrolytes in electric fields. J. Chem. Phys. 2009; 131:234905. [PubMed: 20025346]
75. Salieb-Beugelaar GB, Dorfman KD, van den Berg A, Eijkel JCT. Electrophoretic separation of DNA in gels and nanostructures. Lab Chip. 2009; 9:2508–2523. [PubMed: 19680576]
76. Netz RR. Polyelectrolytes in electric fields. J. Phys. Chem. B. 2003; 107:8208–8217.

77. Manning G. The molecular theory of polyelectrolyte solutions with applications to the electrostatic properties of polynucleotides. Quar. Rev. Biophys. 1978; 11:179–246.

78. Record MT Jr, Anderson CF, Lohman TM. Thermodynamic analysis of ion effects on the binding and conformational equilibria of proteins and nucleic acids: the roles of ion association or release, screening, and ion effects on water activity. Quar. Rev. Biophys. 1978; 11:103–178.

79. Tirado MM, López Martínez CL, García de la Torre J. Comparison of theories for the translational and rotational diffusion coefficients of rod-like macromolecules. Application to short DNA fragments. J. Chem. Phys. 1984; 81:2047–2052.

80. Fernandes MX, Ortega A, López Martinez MC, García de la Torre J. Calculation of hydrodynamic properties of small nucleic acids from their atomic structure. Nucleic Acids Res. 2002; 30:1782–1788. [PubMed: 11937632]

81. Wegener WA. Diffusion coefficients for rigid macromolecules with irregular shapes that allow rotational-translational coupling. Biopolymers. 1981; 20:303–326.

82. Harvey SC. Transport properties of particles with segmental flexibility. I.Hydrodynamic resistance and diffusion coefficients of a freely hinged particle. Biopolymers. 1979; 18:1081–1104.

83. García Molina JJ, López Martínez MC, García de la Torre J. Computer simulation of hydrodynamic properties of semiflexible macromolecules: randomly broken chains, wormlike chains, and analysis of properties of DNA. Biopolymers. 1990; 29:883–900. [PubMed: 2369619]

84. Mellado P, Iniesta A, Diaz FG, García de la Torre J. Diffusion coefficients of segmentally flexible macromolecules with two subunits: a study of broken rods. Biopolymers. 1988; 27:1771–1786. [PubMed: 3233330]

85. Stellwagen E, Muse JM, Stellwagen NC. Monovalent cation size and DNA conformational stability. Biochemistry. 2011; 50:3084–3094. [PubMed: 21410141]

86. Leroy JL, Charretier E, Kochoyan M, Guéron M. Evidence from base-pair kinetics for two types of adenine tract structures in solution: their relation to DNA curvature. Biochemistry. 1988; 27:8894–8898. [PubMed: 3233210]

87. Snoussi K, Leroy LL. Alteration of A·T base-pair opening kinetics by the ammonium cation in DNA A-tracts. Biochemistry. 2002; 41:12467–12474. [PubMed: 12369837]

88. Reinert K-E. Counterion-type characteristic effects on intrinsic bending components of calf thymus DNA; hydrodynamic investigations. J. Biomolec. Struct. Dyn. 1993; 10:991–1000.

89. Manning GS, Ray J. Counterion condensation revisited. J. Biomol. Struct. Dyn. 1998; 16:461–476. [PubMed: 9833682]

90. Ray J, Manning GS. Counterion and coion distribution functions in the counterion condensation theory of polyelectrolytes. Macromolecules. 1999; 332:4588–4595.

91. Bai Y, Greenfeld M, Trvers KJ, Chu VB, Lipfert J, Doniach S, Herschlag D. Quantitative and comprehensive decomposition of the ion atmosphere around nucleic acids. J. Am. Chem. Soc. 2007; 129:14981–14988l. [PubMed: 17990882]

92. Kirmizialtin S, Pabit SA, Meisburger SP, Pollack L, Elber R. RNA and its ionic cloud: solution scattering experiments and atomically detailed simulations. Biophys. J. 2012; 102:819–828. [PubMed: 22385853]

93. Spiriti J, Kamberaj H, de Graff AMR, Thorpe MF, van der Vaart A. DNA bending through large angles is aided by ionic screening. J. Chem.Theory Comput. 2012; 8:2145–2156.

94. Kosikov KM, Gorin AA, Lu X-J, Olson WK, Manning GS. J. Am. Chem. Soc. 2002; 124:4838–4847.

95. Manning GS, Ebralidse KK, Mirzabekov AD, Rich A. An estimate of the extent of folding of nucleosomal DNA by laterally asymmetric neutralization of phosphate groups. J. Biomol. Struct. Dyn. 1989; 6:877–889. [PubMed: 2590506]

96. Manning GS. Comments on selected aspects of nucleic acid electrostatics. Biopolymers. 2003; 69:137–143. [PubMed: 12717728]

97. Manning GS. The contribution of transient counterion imbalances to DNA bending fluctuations. Biophys. J. 2006; 90:3208–3215. [PubMed: 16461401]

98. Skolnick J, Fixman M. Electrostatic persistence length of a wormlike polyelectrolyte. Macromolecules. 1977; 10:944–948.

99. Chen H, Meisburger SP, Pabit SA, Sutton JL, Webb WK, Pollack L. Ionic strength-dependent persistence lengths of single-stranded RNA and DNA. Proc. Natl. Acad. Sci. 2012; 109:799–804. [PubMed: 22203973]
100. Segal E, Widom J. Poly(dA:dT) tracts: major determinants of nucleosome organization. Curr. Opin. Struct. Biol. 2009; 19:65–71. [PubMed: 19208466]
101. Rohs R, West SM, Sosinsky A, Liu P, Mann RS, Honig B. The role of DNA shape in protein-DNA recognition. Nature. 2009; 461:1248–1253. [PubMed: 19865164]
102. Park Y-W, Breslauer KJ. A spectroscopic and calorimetric study of the melting behaviors of a "bent" and a "normal" DNA duplex: $[d(GA_4T_4C)]_2$ versus $[d(GT_4A_4C)]_2$. Proc. Natl. Acad. Sci. USA. 1991; 88:1551–1555. [PubMed: 1996356]
103. Chan SS, Austin RH, Mukerji I, Spiro TG. Temperature-dependent ultraviolet resonance Raman spectroscopy of the premelting state of dA·dT DNA. Biophys. J. 1997; 72:1512–1529. [PubMed: 9083657]
104. Jerkovic B, Bolton PH. The curvature of dA tracts is temperature dependent. Biochemistry. 2000; 39:12121–12127. [PubMed: 11015189]
105. Mukerji I, Williams AP. UV resonance Raman and circular dichroism studies of a DNA duplex containing an A_3T_3 tract: evidence for a premelting transition and threecentered H-bonds. Biochemistry. 2002; 41:69–77. [PubMed: 11772004]
106. Augustyn KE, Wojtuszewski K, Hawkins ME, Knutson JR, Mukerji I. Examination of the premelting transition of DNA A-tracts using a fluorescent adenosine analogue. Biochemistry. 2006; 45:5039–5047. [PubMed: 16605272]
107. Herrera JE, Chaires JB. A premelting conformational transition in poy(dA)-poly(dT) coupled to daunomycin binding. Biochemistry. 1989; 28:1993–2000. [PubMed: 2719942]
108. Manning GS. Limiting laws and counterion condensation in polyelectrolyte solutions. 7. Electrophoretic mobility and conductance. J. Phys. Chem. 1981; 85:1508–1515.
109. Stellwagen E, Stellwagen NC. Probing the electrostatic shielding of DNA with capillary electrophoresis. Biophys. J. 2003; 84:1855–1866. [PubMed: 12609887]
110. Drak J, Crothers DM. Helical repeat and chirality effects on DNA gel electrophoretic mobility. Proc. Natl. Acad. Sci. USA. 1991; 88:3074–3078. [PubMed: 2014227]
111. Niederweis M, Lederer T, Hillen W. Matrix effects suggest an important influence of DNA-polyacrylamide interactions on the electrophoretic mobility of DNA. J. Biol. Chem. 1994; 269:10156–10162. [PubMed: 8144517]
112. Stellwagen NC. DNA mobility anomalies are determined primarily by polyacrylamide gel concentration, not gel pore size. Electrophoresis. 1997; 18:34–44. [PubMed: 9059818]
113. Stellwagen NC. Sequence-dependent bending in plasmid pUC19. Electrophoresis. 2003; 24:3467–3475. [PubMed: 14595693]
114. Lavery R, Pullman B, Zakrzewska K. Intrinsic electrostatic properties and base sequence effects in the structure of oligonucleotides. Biophys. Chem. 1982; 15:343–351. [PubMed: 7115887]

A

0: AGCCTAGCCT ATGACATGAC ACGTTACGAC CAGACCAGCT GCACTGCAGA

CTGGACTGAC GCTAGCTGAC TGTACTGTAT GCAATGCAAC CTCACCTC

1: AGCCTAGCCT ATGACATGAC ACGTTACGAC CAGACCAGCT GCACTGCAGA

CTGGGCC**AA AAAA**GCTGAC TGTACTGTAT GCAATGCAAC CTCACCTC

2i: AGCCTAGCCT ATGACATGAC ACGTTACGAC CAGACCAGCT GCACGGCG**AA**

AAAAGCCG**AA AAAA**GCTGAC TGTACTGTAT GCAATGCAAC CTCACCTC

3i: AGCCTAGCCT ATGACATGAC ACGTTACGAC CAGAGCGC**AA AAAA**GGCG**AA**

AAAAGCCG**AA AAAA**GCTGAC TGTACTGTAT GCAATGCAAC CTCACCTC

4i: AGCCTAGCCT ATGACATGAC ACGCG**AAAAA A**GCGC**AAAAA A**GGCGCCGGC

AAAAAGCCG AAAAAACGAC TGTACTGTAT GCAATGCAAC CTCACCTC

2i/o: AGCCTAGCCT ATGACATGAC ACGCG**AAAAA** AGCGC**AAAAA** AGGCGCCGGC

AAAAAAGCCG **AAAAAA**GAC TCTACTGTAT GCAATGCAAC CTCACCTC

4o: AGCCTAGCCT ATGACATGAC **AAAAAA**GCGC ACGCG**AAAAA A**GGCGCCGGC

AAAAAAGCCG TACCG**AAAAA A**GCACTGTAT GCAATGCAAC CTCACCTC

B

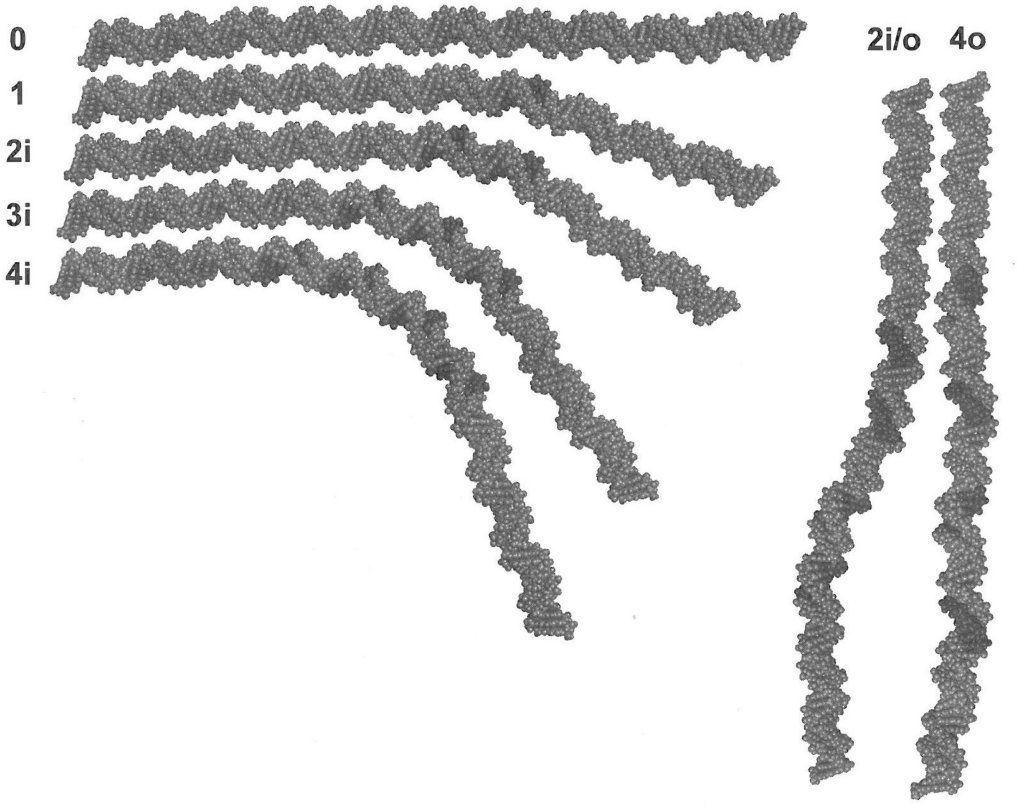

Figure 1.

(A), Sequences of the 98-base pair DNA constructs used in this work. The names of the first four sequences (samples 0 to 4i) indicate the number of in-phase A_6-tracts in the sample. Sample 2i/o contains two pairs of in-phase A-tracts, with each pair out-of-phase with the other pair. Sample 4o (out-of-phase) has four A_6-tracts that are separated by 16 residues, making them out of phase with each other. The A_6-tracts in each fragment are shown with a larger font for clarity. (B), Representations of 3-dimensional structures of the 98-bp constructs. Standard PDB files were generated from the model.it server.[54] This server uses input sequence data to generate DNA structures based on consensus trinucleotide parameter sets from DNAse I digestion and nucleosome positioning data.[55] Molecular models were rendered from these PDB files with PyMOL (DeLano Scientific).

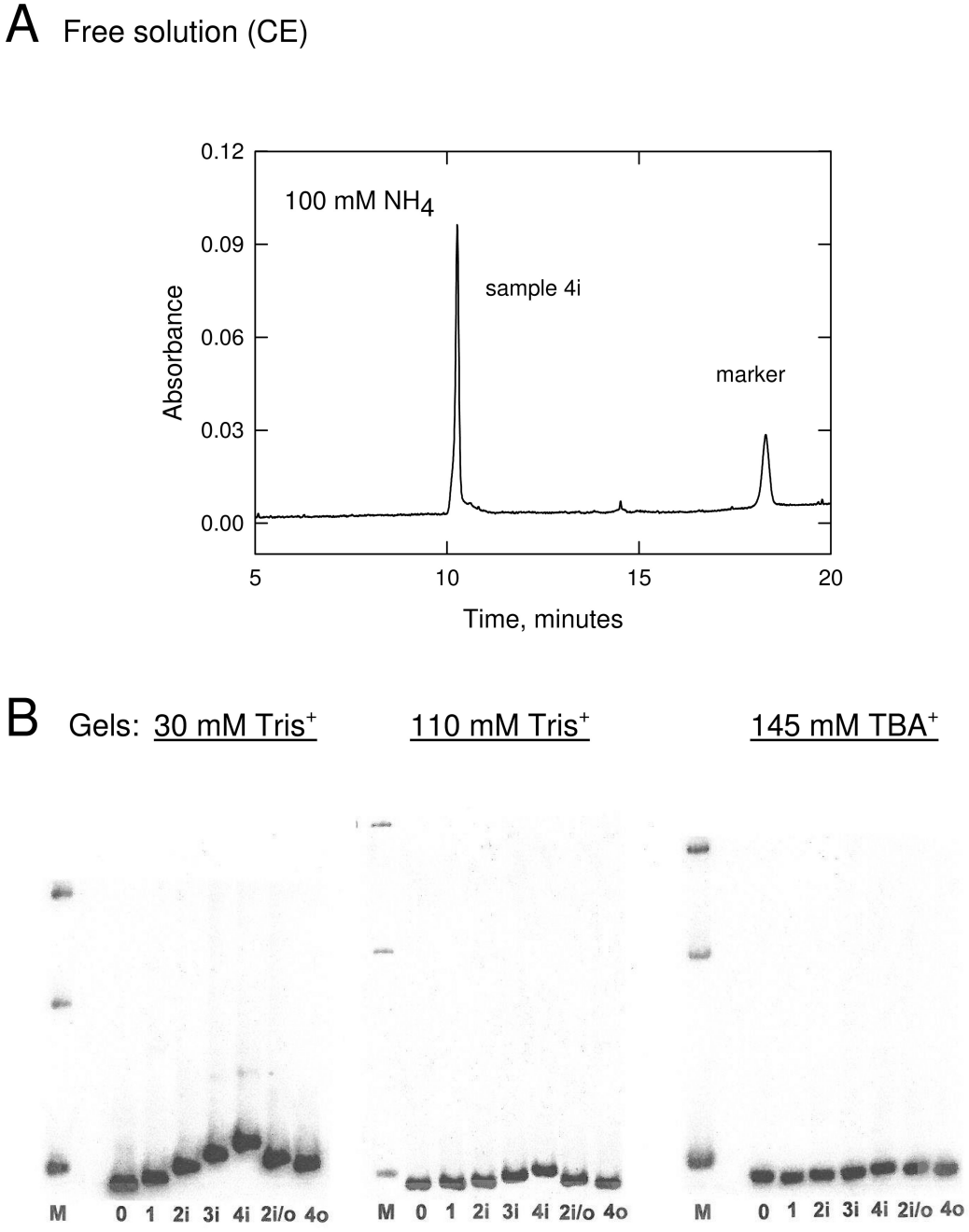

Figure 2.

Typical electropherograms observed for A-tract samples. (A), CE electropherogram observed for sample 4i in a BGE containing 100 mM NH_4^+ ions. The absorbance (254 nm) is plotted as a function of the time elapsed after the electric field is turned on. The peak on the left corresponds to sample 4i, the peak on the right corresponds to the marker ACCTGAT. (B), Electropherograms observed for the A-tract-samples in polyacrylamide gels cast and run in: (left), 30 mM $Tris^+$; (center), 110 mM $Tris^+$; and (right), 145 mM TBA^+. The DNA samples are identified at the bottom of each lane. The lane marked M corresponds to the 100-bp ladder; the bands corresponding to the 300-, 200- and 100- bp fragments (top to bottom) are shown.

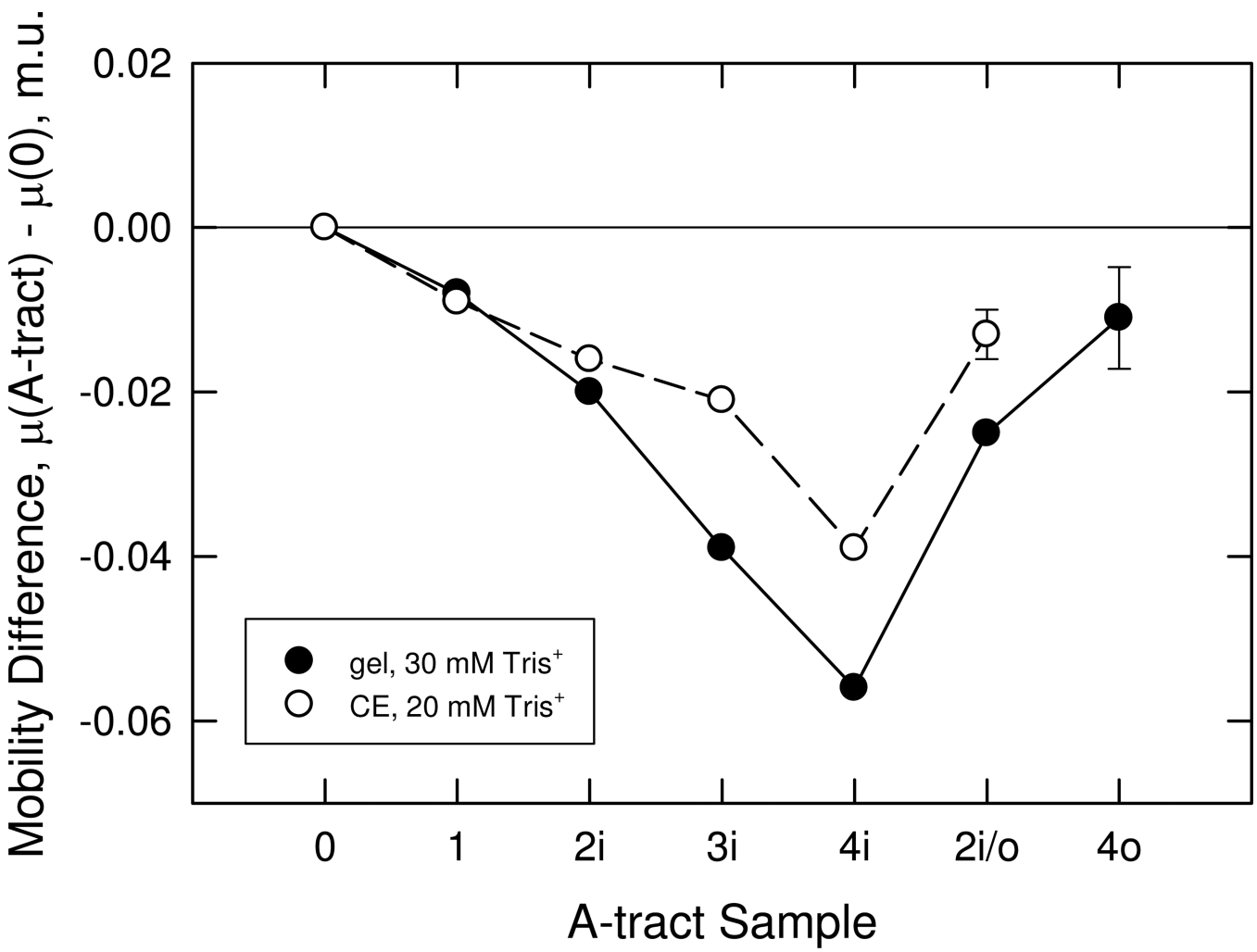

Figure 3.

Comparison of the mobility differences observed for the A-tract samples in free solution and in polyacrylamide gels. The difference in mobility between the A-tract sample and sample 0, with no A-tracts, is plotted as a function of the number and arrangement of the A-tracts. (●), Gel mobility differences observed 30 mM $Tris^+$; and (○), free solution (CE) mobility differences observed in 20 mM $Tris^+$. In this and subsequent figures, the average standard deviation of the mobility differences, determined by replicate measurements, are indicated by error bars attached to one of the data points. The lines are drawn to guide the eye.

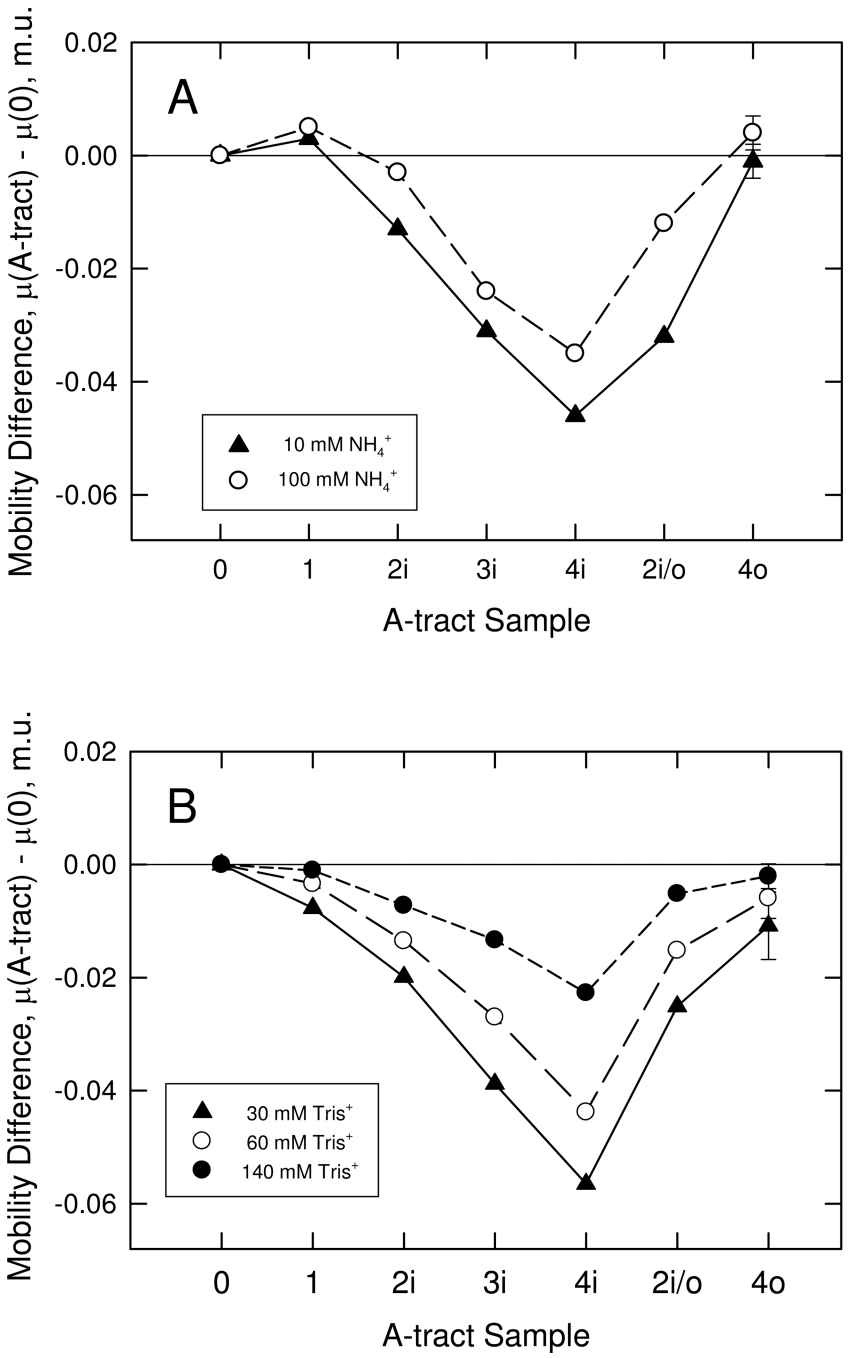

Figure 4.

Mobility differences observed for the A-tract samples in BGEs containing different concentrations of hydrophilic cations. (A), Free solution (CE) mobility differences observed in BGEs containing: (▲), 10 mM; or (o), 100 mM NH_4^+ ions. (B), Gel mobility differences observed in BGEs containing: (▲), 30 mM; (○), 60 mM; or (●), 140 mM $Tris^+$ ions. The lines are drawn to guide the eye.

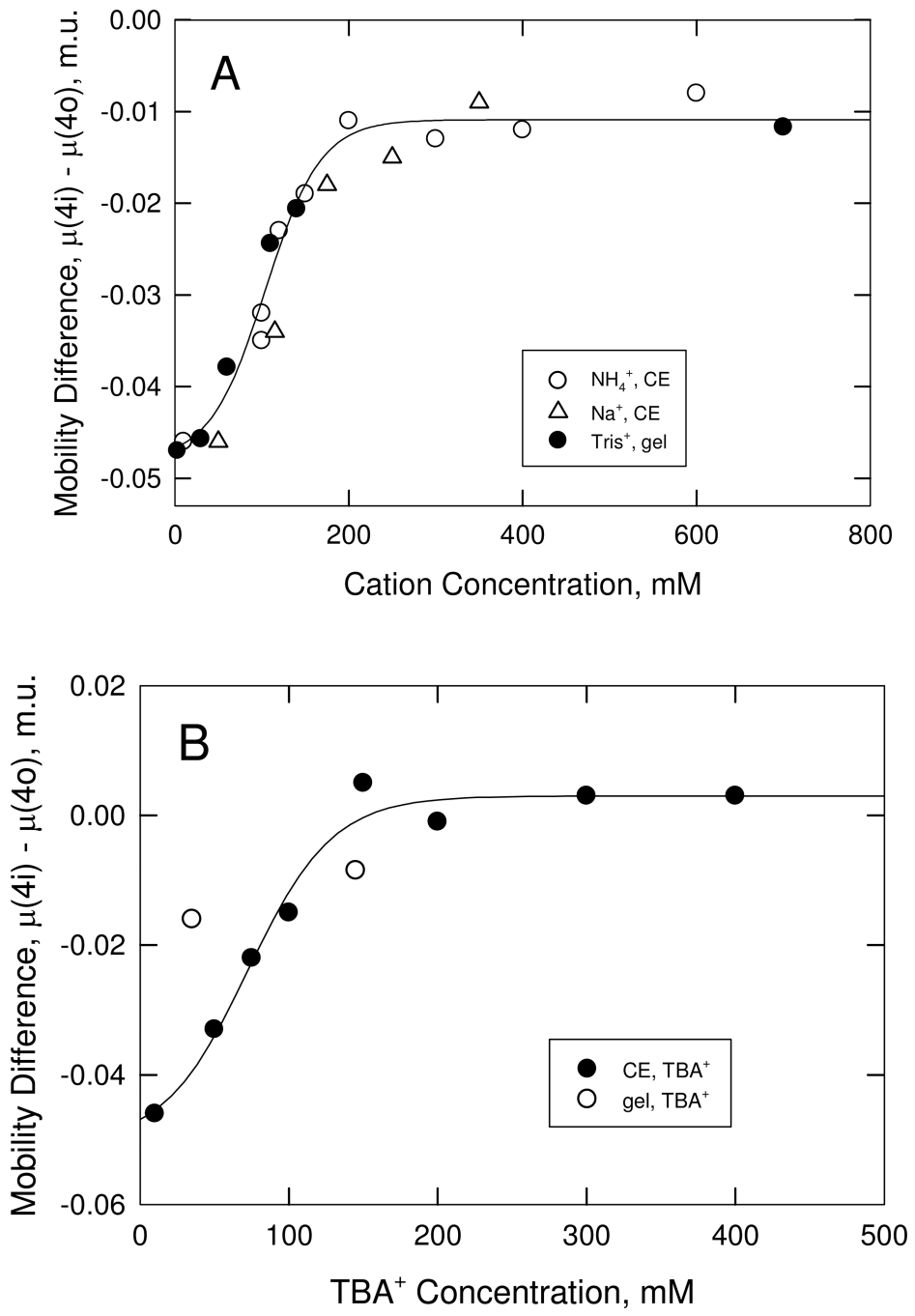

Figure 5.

Dependence of the mobility difference between samples 4i and 4o, μ(4i) – μ(4o), on cation concentration. (A), Hydrophilic cations. Free solution (CE) mobility differences observed in BGEs containing (○), NH_4^+ ions; or (Δ), Na^+ ions; and gel mobility differences observed in BGEs containing (●), $Tris^+$ ions. The combined data sets were fit with a 4 parameter sigmoid with a plateau value of −0.011 ± 0.003 m.u. and a midpoint of 104 ± 7 mM (r^2 = 0.977). (B), Tetrabutylammonium ions. (●), Free solution (CE) mobility differences; and (○), gel mobility differences. The curved line corresponds to the fit of a four parameter sigmoid to the free solution mobility differences, assuming that the mobility difference observed in 10 mM NH_4^+ is also valid for 10 mM TBA^+. For technical reasons

(deterioration of peak shape), the free solution mobility differences could not be measured at very low [TBA^+]. The plateau value of the mobility difference at high [TBA^+] is 0.003 ± 0.009 m.u.; the midpoint of the transition occurs at 73 ± 12 mM (r^2 = 0.980).

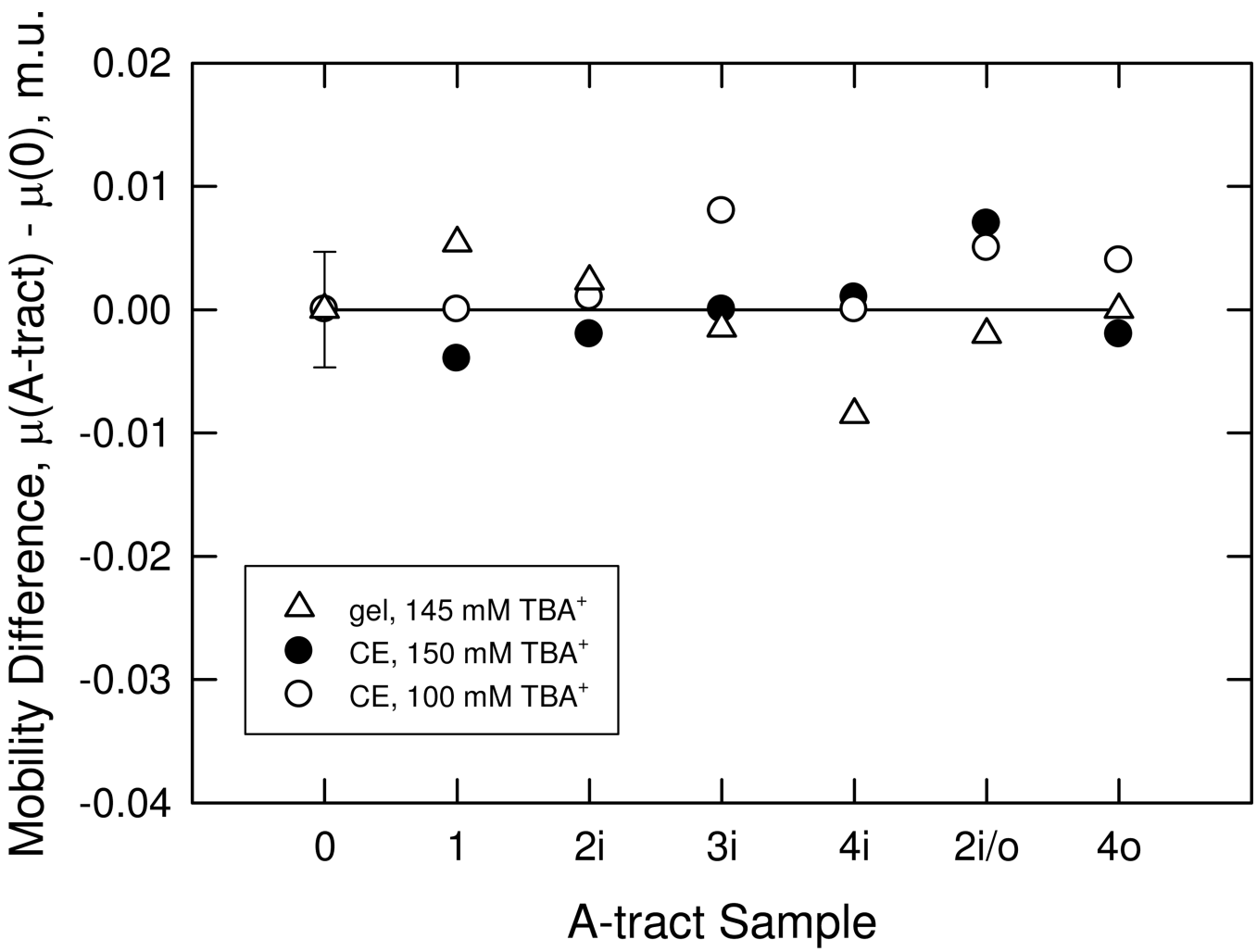

Figure 6.

Mobility differences observed for the A-tract samples in BGEs containing TBA^+ ions. Free solution (CE) mobility differences observed in: (o), 100 mM; and (●), 150 mM TBA^+; and (Δ), gel mobility differences observed in 145 mM TBA^+. The solid line corresponds to the average mobility difference for all samples, 0.000 ± 0.005 m.u.